The Laser Speckle Shift Strain Measurement System

L.C. Greer and L.G. Oberle
National Aeronautics and Space Administration
Lewis Research Center
Cleveland, Ohio 44135

ABSTRACT

The objective of this project is to develop a strain measurement system for small diameter wires and fibers at elevated temperatures using Yamaguchi's laser-speckle strain measurement technique. Previous work done by NASA Lewis colleagues John P. Barranger and Christian T. Lant demonstrated that Yamaguchi's technique can be used to accurately measure strain in fibers as small as 21 microns (1 mil) in diameter. The next step in the project development is to create a robust version of this system that is both reliable and easy to use in a laboratory environment. After deciding that a post-processing system would best suit the design criteria, we realized that special hardware was needed to record the speckle patterns at real-time rates for the duration of the experiment. Specialized hardware would also be required to process the large volume of image data in a reasonable amount of time. The final design is centered around an image processing unit which performs video operations at real time rates. A central computing unit works in tandem with the image processor to coordinate the operations of the image processor with the operations of a tensile test frame and various optical components. This system is capable of recording speckle patterns to disk at the RS-170 frame rate (30 frames per second) for tests lasting a few hours. Furthermore, the system tracks the movement of the correlation peak with minimal error, allows easy variation of acquisition and correlation computation parameters and performs the thousands of correlations necessary to compute the strain in a reasonable amount of time. Lastly, the system provides a simple user interface to facilitate its use in the laboratory.

INTRODUCTION

The Applications Group within the Instrumentation and Control Technology Division of NASA Lewis Research Center is currently focussing its efforts on designing and constructing a non-contact strain measurement system capable of extracting strain data along one principal axis from fibers at elevated temperatures. Past techniques for measuring strain in test specimens utilized extensometers or markers for visual observation. These techniques lack the proper gage length and/or resolution to accurately determine the strain in fibers. Consequently, we have elected to base our system on the laser speckle-shift strain measurement technique of Yamaguchi.[1] This technique allows strain measurements in the presence of rigid-body motion with resolutions of about 15 $\mu\epsilon$. In addition, this technique requires no surface preparation, and can make strain measurements at elevated temperatures. Finally, the system operates in a post-processing mode which allows data acquisition at maximum rates and adds flexibility to the strain calculations. This paper describes the system design and discusses the results obtained during the trial runs of the system.

THEORY

Laser-speckle strain measurement relies upon a shifting interference pattern (speckle pattern) resulting from the surface deformation of a laser illuminated optically diffuse specimen under varying load conditions. The surface deformation of the specimen is described by vector $a(x,y)$, and the resulting shift in the speckle pattern is given by vector $A(X,Y)$ (figure 1). The geometry of the optical setup shows the camera plane and the specimen plane separated by a distance L_o. A laser beam with a radius of curvature defined as L_s travels in the x-z plane, and intersects the specimen surface at an incident angle of θ_i. The translational forms of rigid-body motion (a_x, a_y, a_z) are components of the surface deformation vector $a(x,y)$. It should be noted that the specimen can also rotate about the x, y or z axes. These rotational components of rigid-body motion are defined by Ω_x, Ω_y and Ω_z. Figure 1 shows the left half of a second specimen plane which has a rotational component about the y-axis.

When the speckle displacement is viewed from a plane parallel to the specimen surface (perpendicular to the plane of incidence) at a distance L_o which is much smaller than the beam's radius of curvature L_s, and when the spot diameter ω of the incident beam is much smaller than L_o, the speckle displacements reduce to the expressions shown in equations [1a] and [1b].[2] Now the

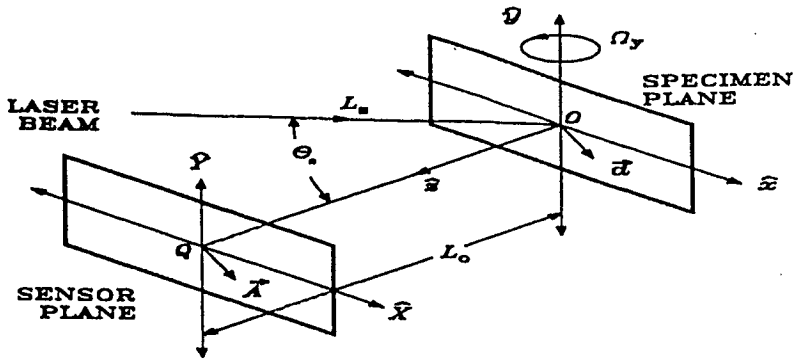

Figure 1 Simplified Coordinate System

relationship between the speckle shift and the strain terms (ϵ_{xx} – the x component of the strain tensor, and ϵ_{xy} – the shear component of the strain tensor) becomes apparent.

$$A_x = a_x - L_o(e_{xx}\sin\theta_s - \Omega_y(\cos\theta_s + 1)) \tag{1a}$$

$$A_y = a_y - L_o(e_{xy}\sin\theta_s - \Omega_x(\cos\theta_s + 1) - \Omega_z\sin\theta_s) \tag{1b}$$

If the speckle displacement A_y is much less than the sum of the camera's pixel height and the speckle size ($1.22\lambda L_o/\omega$), then A_x can be determined by cross-correlating an image line from the specimen's speckle pattern before surface deformation (reference frame) with the same image line after surface deformation (current frame). The correlation between the reference frame and current frame is actually obtained from a subset or window of points within each image line. The window width W is selected such that a window centered in the image line will move to the extremes of the image line when subjected to the maximum speckle displacement $\pm\Delta x_{max}$. This is illustrated by figure 2 where the box centered horizontally along the image line represents the window with width W. The remaining portion of the image line to each side of the window represents the maximum speckle displacement $\pm\Delta x_{max}$ which is the most the window could move before its edge would move beyond the image line.

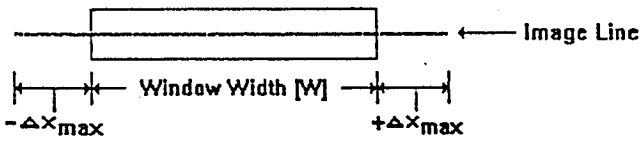

Figure 2: Window within image line

The speckle displacement Δx at the peak amplitude of the cross-correlation R yields the value of A_x (equation [2]).

$$A_x = \Delta x \text{ at } MAX(R_{\theta_s}),\quad R_{\theta_s}(\Delta x) = \frac{1}{W}\int_0^W F_{\theta_s}(x)G_{\theta_s}(x+\Delta x)dx,\quad -\Delta x_{max} \le \Delta x \le +\Delta x_{max} \tag{2}$$

W=window width, Δx=speckle displacement
$F_{\theta_s}(x)$ *=reference frame*
$G_{\theta_s}(x+\Delta x)$ *=current frame*

Cancellation of the translational component a_x and the rotational component Ω_y in A_x (equation [1a]) is accomplished by taking the difference between speckle displacements from two opposing beams located at $-\theta_s$ and θ_s.
The speckle shift ΔA_x is the amount of shift Δx at the cross-correlation peak of one beam (MAX$\{R_{\theta_s}\}$) subtracted from the amount of shift at the cross-correlation peak of the opposing beam (MAX$\{R_{\theta_s}\}$).

$$\Delta A_x = A_x(\theta_s) - A_x(-\theta_s) = -2L_o e_{xx} \sin|\theta_s| \tag{3}$$

$$\Delta A_x = (\Delta x \text{ at } MAX(R_{\theta_s})) - (\Delta x \text{ at } MAX(R_{-\theta_s})) \tag{4}$$

It follows from equation [3] that the strain at the point of incidence of the beam can be defined as a function of the speckle shift. The following expression reveals this linear relationship between the strain ϵ_{xx} and the speckle shift ΔA_x.

$$e_{xx} = \frac{-\Delta A_x}{2L_o \sin|\theta_s|} \tag{5}$$

Cancellation of rigid-body motion is incomplete if the distance L_o is not much smaller than L_s. To account for the error introduced by the radius of curvature of the beam at the specimen location, an extra term is added to equation [5].

$$e_{xx} = \frac{-\Delta A_x}{2L_o \sin|\theta_s|} - \frac{a_z \cos|\theta_s|}{L_s} \tag{6}$$

It becomes obvious from the above expression that a means must be provided to position the specimen at the beam waist where the radius of curvature approaches infinity and the error term becomes negligible.

SYSTEM DESIGN

The system, as shown in figure 3a, contains five major components; a central computer (386 33Mhz Personal Computer), a screw driven tensile test machine (Instron 4502), an image processing unit (RCI Trapix Plus Unit), a CCD (charge-coupled device) array camera (COHU 6500), and optical hardware (acousto-optic modulator, Pockels Cell, etc). All communication between individual components is channeled through the central computer which is equipped with an IEEE interface card (National Instruments AT-GPIB) and a data acquisition card (Data Translation DT2801-A) complete with A/D, D/A and binary I/O capability. The system timing originates from the vertical retrace and odd/even signals from the camera which keeps the image acquisition, load/extension readings and cross-head movement of the tensile test machine synchronized.

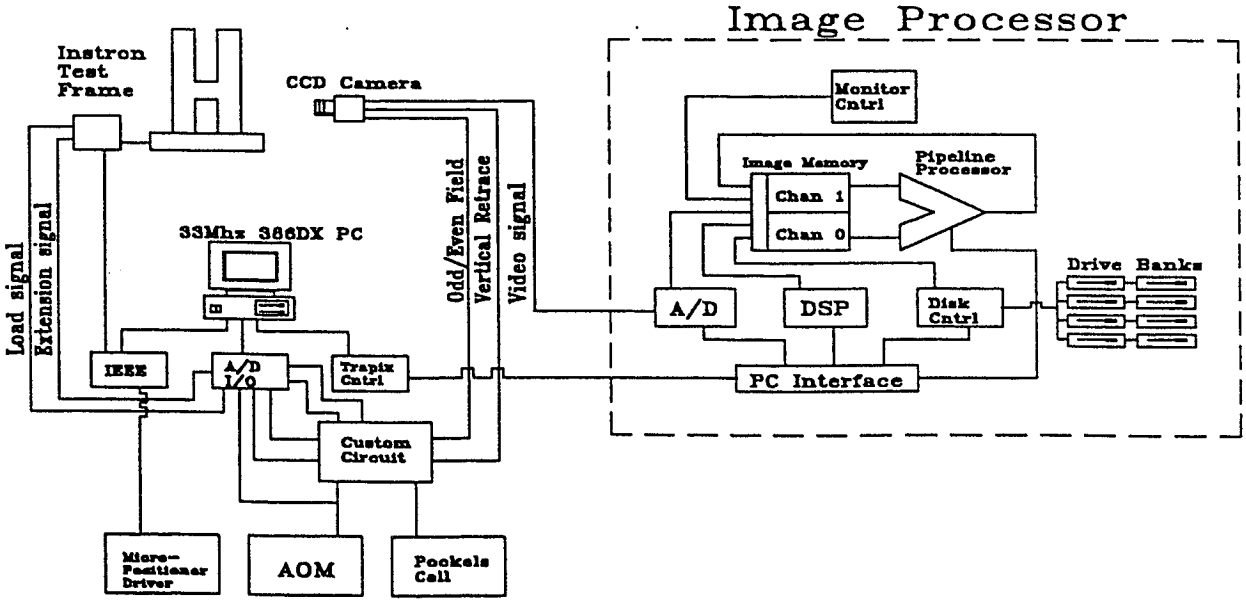

Figure 3a: Laser speckle system

The optical system initially illuminates the specimen with one beam at an incident angle of θ_x, then the beam is blanked by the acousto-optic modulator while the Pockels Cell twists the polarity of the beam enough to cause the polarized beam-splitter cube to blank the first beam and allow the second beam to illuminate the specimen at an incident angle of $-\theta_x$ (figure 3b). This cycle is synchronized to the frame rate (30 Hz) of the camera, therefore consecutive frames remain locked to alternate beams. The blanking signal for the acousto-optic modulator is derived by 'anding' the vertical retrace and odd/even signals. The resulting output signal triggers a variable length time delay circuit (555 in monostable configuration) that allows the user to select the width of the blanking pulse. The upper/lower beam signal to the Pockels Cell is derived by using the falling edge of the odd/even signal to toggle the output of a flip-flop.

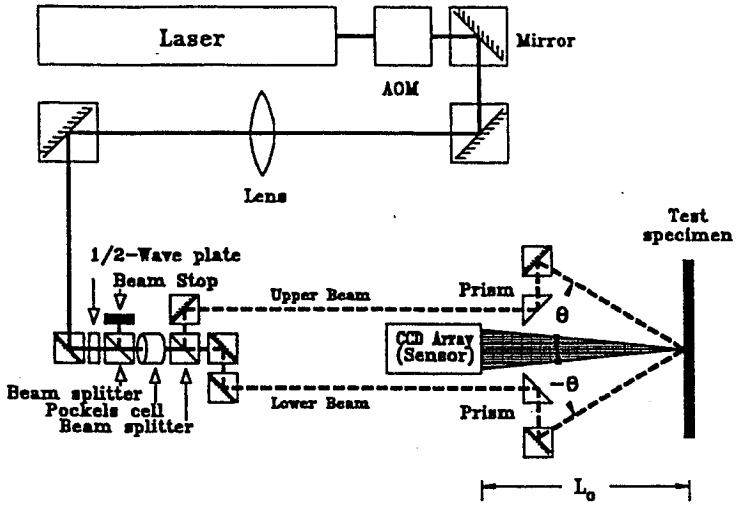

Figure 3b: Optical layout

The acquisition sequence is as follows. First, the A/D card is setup to monitor the upper/lower beam signal to the pockels cell driver. Using its internal clock which is set to ten times the frequency of the upper/lower beam signal, it polls for a rising edge transition. Upon finding a rising edge transition, it resets itself to monitor the channels for load and extension using the vertical retrace signal as an external clock and a mid-frame start signal as an external trigger. The image processor is then signalled to begin acquiring images on the next frame cycle which happens to be the upper beam image frame. The user can also initiate the process on the lower image frame by polling for a falling edge transition. The image processor fills an image bank while the A/D card which is operating in dual DMA transfer mode simultaneously fills an array in the PC memory with load/extension data. A 1k line is left open in the image bank for the data held in the load/extension array. The image processor contains two banks of image memory (Channels 0 and 1) which allow dual operations to occur simultaneously. While the camera is dumping images to one bank of image memory, the previous images stored in the second bank of image memory is being dumped to disk. This allows several lines from each speckle image to be captured and recorded to disk at the RS-170 frame rate. Once recorded, the speckle image can be replayed in real time or correlated. Initially it was thought that the multiple lines provided by the CCD array would be used for a correlation along the y-axis. This would add the capability of tracking a specific line within the speckle pattern which normally moves along the y-axis because of rigid-body motion. Without this capability, flat plate specimens with excessive y-axis rigid-body motion would decorrelate rapidly because the speckle pattern varies dramatically along the y-axis (vertical direction in figure 4a). However, it has been observed that a specimen with a physical dimension less than the beam spot size ω, such as a fiber or wire, generates elongated speckle patterns along the direction of the smaller dimension (figure 4b). This effect is caused by diffraction. In our system, the elongated speckles reduce sensitivity to rigid-body motion along the y-axis which eliminates the need to track the correlation line. Nevertheless, several lines acquired by the CCD array are stored. These lines could prove useful for large specimens where line tracking might be required and for future design ideas which might utilize multiple lines for the correlation.

In order to increase the speed of the correlation, a pipeline processor in the image acquisition unit is used to perform all of the correlation multiplications. The pipeline processor can multiply two 1k-by-1k 8-bit images resulting in a 1k-by-1k 16-bit product in one frame period (1/30th of a second).[3] Therefore by filling one 1k-by-1k image with several smaller image blocks made

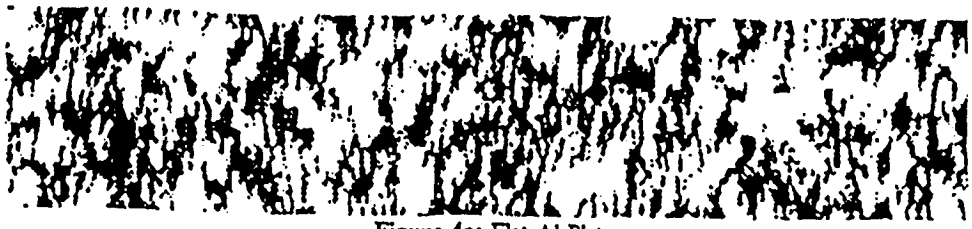

Figure 4a: Flat Al Plate

Figure 4b: 75μm W-Re

of $2\Delta x_{max}$ stacked replicas of an unshifted line from the current reference speckle pattern frame ($F\{x\}$) (figure 5a) and by filling the remaining 1k-by-1k image with several smaller image blocks made of stacked incrementally-shifted replicas of the corresponding line from a displaced speckle pattern frame ($G\{x+\Delta x\}$ from $-\Delta x_{max}$ to Δx_{max}) (figure 5b), all of the products ($F\{x\}G\{x+\Delta x\}$ from $-\Delta x_{max}$ to Δx_{max}) in the correlation integral (equation [2]) are obtained for several frames in 1/30th of a second. Figures 5a and 5b show how a reference and source (displaced speckle pattern) image block is produced from a single line taken from the respective reference and source frames. Each image block in the 1k-by-1k source image is generated from a new source frame whereas the number of frames used to produce the image blocks in the 1k-by-1k reference image depends upon the frequency of reference updates. After taking the product, the digital signal processor (DSP) onboard the image processor unit sums the products of all x values and finds the peak mean amplitude among all Δx values.

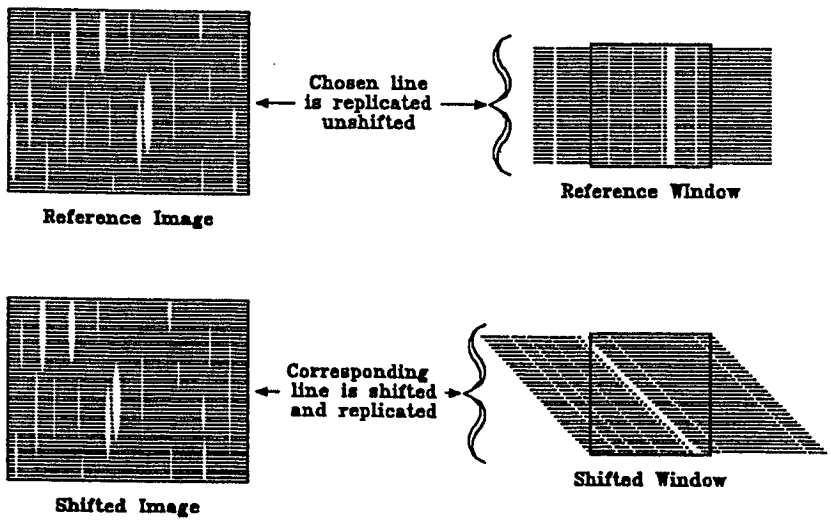

Figures 5a & 5b Reference and source multiplication

Accurately tracking the correlation peak in the presence of erratic speckle-pattern fluctuation has proven to be the most challenging aspect of the system design. The current peak-tracking techniques used in our system utilize limits within the speckle displacement range and correlation peak thresholds for determining when to update the reference from a new frame or when to slide along the current reference frame. If at any time the amplitude of the correlation peak *MAX(R)* falls below a user specified threshold, a reference from a new frame is obtained. Also if the cumulative speckle displacement within the current reference frame exceeds the maximum allowable speckle displacement per reference frame $\pm\Delta x_{max}$, a reference from a new

frame is obtained. Lastly, if the speckle displacement reaches a user specified limit and the cumulative speckle displacement within the current reference is less than the maximum allowable displacement per reference frame, the current reference frame is shifted to match the displacement of the current speckle pattern.

After tracking the speckle shift of each beam for the duration of the experiment, the difference between the shifts for each time slot is multiplied by the constant given by $(pixel\ width)/2L_o sin(\theta_o)$. This yields the strain record of the experiment which is plotted against the load record of the experiment. All plots available to the user, such as the load-extension curve and the load-strain curve, have automatic and manual scaling modes. Furthermore, a linear-regression algorithm is included to determine Young's Modulus from the slope of the stress-strain curve. The user selects the region of the curve to perform the linear-regression and the routine returns the modulus value, y-intercept and correlation coefficient.

RESULTS

Several fibers were tested during the evaluation of the system. Among these fibers were tungsten - 3% rhenium (79μm–3.1mil and 203μm–8mil), sapphire (129μm–5.1mil) and silicon-carbide (141μm–5.6mil). The large diameter fibers and the fibers with a high Young's Modulus could not be adequately pre-loaded with the available 10 Newton load cell. This increased the level of rigid-body motion encountered during the test which created more scatter in the data. One problem created by rigid-body motion can be seen in the error term of equation [6] where the out-of-plane motion a_z contributes to the scatter in the data. Tracking the speckle shift during periods of excessive rigid-body motion usually requires frequent reference updates. With each new reference acquired there is a small element of random error introduced into the cumulative speckle shift record.[4] This error also generates scatter in the strain data. Nevertheless, the stress-strain curves for tungsten-rhenium and sapphire yield a Young's Modulus within one to three percent of the "book value" for these materials. The tungsten-rhenium fiber has the smaller diameter 79μm (3 mil) and the lower modulus (380 GPa "book value", 383 GPa measured) as compared to the sapphire fiber with the larger diameter 129μm (5.1 mil) and higher modulus (450 GPa "book value", 435 GPa measured). As expected from a smaller component of rigid-body motion, the stress-strain curve for the tungsten-rhenium fiber (figure 6) exhibits less scatter than the stress-strain curve of the sapphire fiber (figure 7). Increased pre-loading should help eliminate this scatter in the stress-strain data. Consequently, a 100 newton load cell will be acquired in the near future which will allow adequate pre-loading of the fibers. The offset lines in figures 6 and 7, which have slopes equal to the book value of the modulus for each fiber, are intended to serve as visual comparisons with the slopes of the fitted lines.

CONCLUSION

The laser speckle strain measurement system provides a reliable and relatively simple means for measuring strain on wires and fibers. Ultimately the system will take strain measurements from fibers heated to temperatures around 1000 °C. Future endeavors include creating a miniature unit the uses two different color beams and a real-time correlator which would eliminate the need for the image processing unit. The new system would have a much smaller footprint and would allow for experiments requiring instantaneous strain feedback.

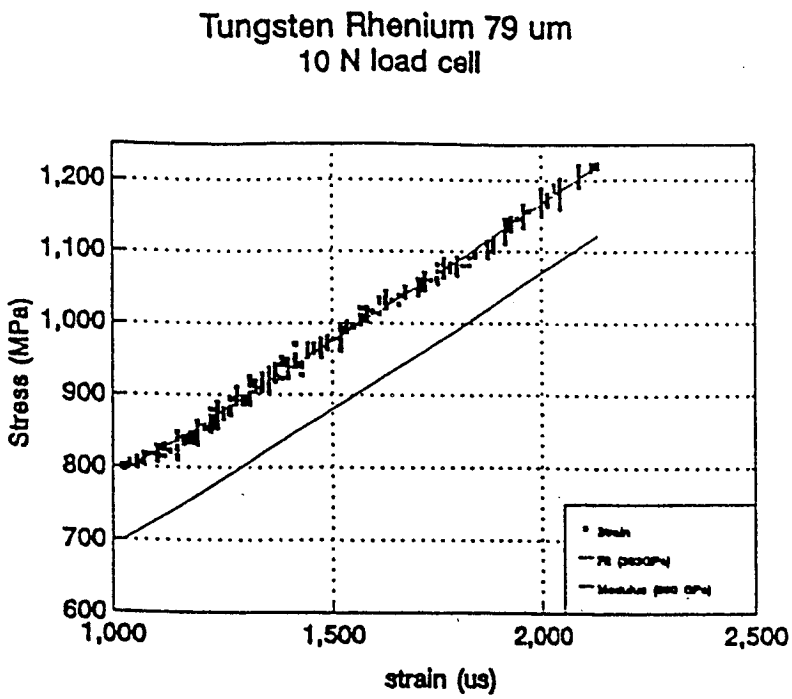

Figure 6: W-Re stress-strain plot

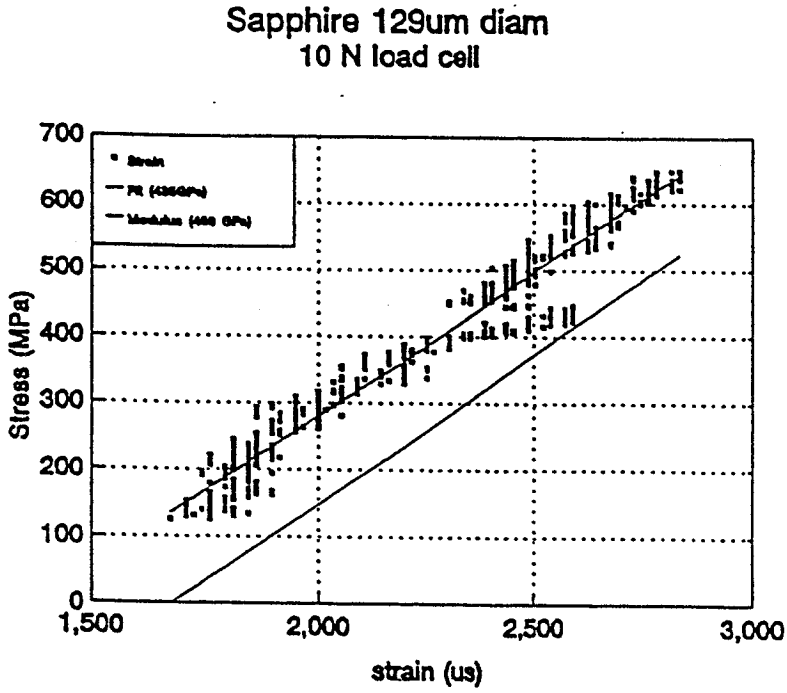

Figure 7: Sapphire stress-strain plot

REFERENCES

1. Yamaguchi, I.: "A Laser-Speckle Strain Gauge", J. Phys. E. Sci. Instrum., vol. 14, no. 11, Nov. 1981, pp. 1270-1273.

2. Lant, C.T.: "Feasibility Study for the Advanced One-dimensional High Temperature Optical Strain Measurement System -- Phase III", Sverdrup Technology, Inc. NASA Contract NAS3-25266, NASA CR 185254, 1990.

3. Recognition Concepts, Inc.: Trapix Plus User's Manual, Document number 905000-001, Jan. 31, 1991, pp. 199-252.

4. Barranger, J.P., Lant, C.T.: "Tradeoffs in Laser-Speckle Strain Measurements", HITEMP Review 1989, NASA Conference Publication 10039, pp. 37.1-37.10.